Published in Journal of Non-Crystalline Solids 266-269, 519-523, 2000
which should be used for any reference to this work

Electron spin resonance and optical characterization of defects in microcrystalline silicon

M. Vaněček [a,*], A. Poruba [a], Z. Remeš [a], J. Rosa [a], S. Kamba [b], V. Vorlíček [b], J. Meier [c], A. Shah [c]

[a] *Institute of Physics, Academy of Sciences of the Czech Republic, Cukrovarnická 10, CZ-16200 Prague 6, Czech Republic*
[b] *Institute of Physics, Academy of Sciences of the Czech Republic, Na Slovance 2, CZ-18221 Prague 8, Czech Republic*
[c] *Institut de Microtechnique, Universite de Neuchatel, rue Breguet 2, CH-2000 Neuchatel, Switzerland*

Abstract

Electron spin resonance (ESR), constant photocurrent method (CPM), photothermal deflection spectroscopy (PDS), Raman and IR spectroscopy have been used to measure microcrystalline silicon films. Besides standard defects with a *g*-value of 2.0055, new defects with a *g*-value ~2.0030 have been created during annealing this material. Proportionality between the subgap optical absorption and ESR spin density has been observed.

1. Introduction

Since the introduction of entirely hydrogenated microcrystalline silicon (μc-Si:H) single junction [1] and amorphous/microcrystalline silicon tandem cells (micromorph cells) [2], similar materials have been obtained by several laboratories [3,4]. As the μc-Si:H is a heterogeneous material, it is important to determine the properties of this 'solar grade' material in terms of microstructure, defect density, transport and optical properties.

Direct observation of material microstructure (by transmission electron microscopy) and study of transport properties is described in other papers of this issue [5,6]. In this paper, we report on parallel measurement of electron spin resonance (ESR) and optical absorption with the aim to correlate the measured spin density with the defect-related subgap absorption.

* Corresponding author. Tel.: +420-2 2031 8540; fax: +420-2 3123 184.
E-mail address: vanecek@fzu.cz (M. Vaněček).

2. Experimental

Layers of μc-Si were deposited in a capacitively coupled parallel plate reactor, using the very high frequency glow discharge (VHF-GD) method [1,2,4], at an excitation frequency of 110 MHz and substrate temperature of 250°C [7]. Under 'device quality conditions', the 2–7 μm thick films were deposited from hydrogen diluted silane on glass (Schott AF45) and c-Si wafers. Flakes, peeled from thicker films, were used for ESR measurements.

Transmittance/reflectance (T/R), constant photocurrent method (CPM) and photothermal deflection spectroscopy (PDS) have been used for the determination of the optical absorption coefficient as a function of photon energy, $\alpha(E)$. Our

theory for the optical measurement on rough layers has been applied for evaluation of the true optical absorption coefficient [8].

A stepwise annealing have been done in an oxygen-free atmosphere (ultra high purity molecular hydrogen), at temperatures from 380°C to 690°C. IR absorption and Raman scattering have been used to monitor hydrogen effusion and structural changes.

3. Results

The typical spin density ($g \cong 2.0055$) in our 'as-grown' undoped μc-Si:H is $\sim 10^{16}$ cm^{-3} as reported in Ref. [9]. These densities were measured either several (2–50) days or more than 1 year after the deposition. The activation energy of the electrical conductivity was typically between 0.6 and 0.3 eV. The changes in ESR spectrum with annealing are distinct, as shown in Fig. 1. Annealing above 400°C creates a new signal with a *g*-value of around 2.0030. Further annealing at higher temperatures increases the intensity of the component with a *g*-value of around 2.0055 (silicon dangling bonds [10]).

The new $g \cong 2.0030$ resonance has usually two components: the first one is 'annealing dependent' and the second, with a smaller *g*-value (2.0026), is 'ambient atmosphere dependent'. In our ESR system, the μc-Si flakes and powder, placed inside a silica tube were flushed with nitrogen gas. Flushing with N increased this second component. When we introduce oxygen instead of nitrogen into the resonator, this second component diminishes, as documented in Fig. 2.

Structural changes with annealing are detected in the IR and Raman spectra, as shown in Figs. 3 and 4. In some samples, an increase at the usually small oxygen band around 1100 cm^{-1} is observed after the first anneal at 400°C and exposure for a few days to air. Raman spectra have three components (Fig. 4). Integrated absorption in the 480 cm^{-1} band decreases with annealing. Correspondingly, the integrated absorption in the smaller width 520 cm^{-1} peak increases and in the 500–505 cm^{-1} shoulder stays approximately constant.

Electrical conductivity, which was in the 'as-grown' state $\sim 10^{-6}$ to 10^{-8} Ω^{-1} cm^{-1}, decreased after anneal at 550°C for 24 h to $\sim 10^{-4}$ Ω^{-1} cm^{-1}.

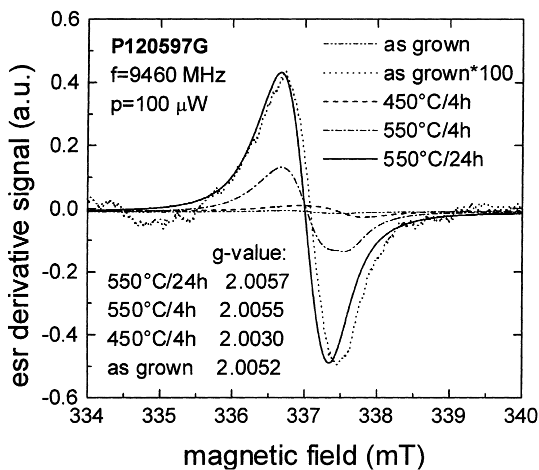

Fig. 1. ESR spectra of μc-Si:H in the 'as-grown' state (dotted curve is 100×expanded) and after successive anneals in ultra-pure molecular hydrogen, for a given annealing temperature and time.

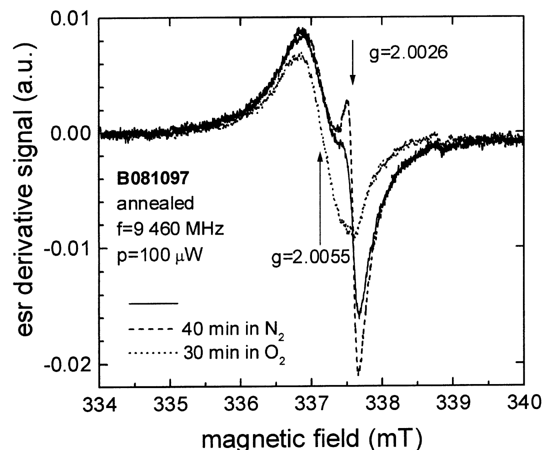

Fig. 2. ESR spectra of another sample after a several successive anneals in the range 400–550°C. Full curve is the measurement immediately after placing the sample into resonator, dashed curve is after 40 min flushing the resonator with nitrogen. The dotted curve is after 30 min of oxygen flow.

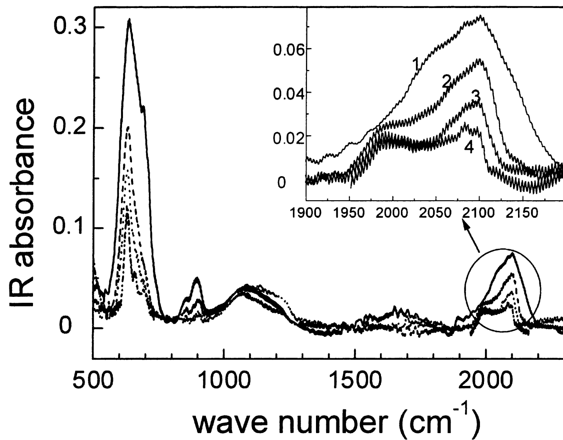

Fig. 3. IR spectra in the 'as-grown' state (1), after successive anneals for 4 h at 400°C (2), 450°C (3) and 550°C (4).

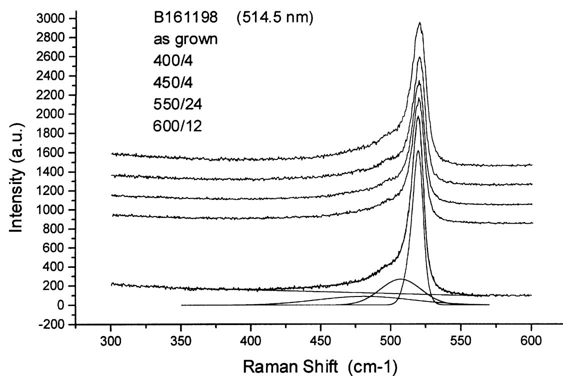

Fig. 4. Raman spectra of μc-Si:H in the 'as-grown' state and after successive anneals for a given temperature/time. Deconvolution of spectrum into three components is also shown.

Simultaneously, with the hydrogen effusion, the optical absorption coefficient $\alpha(E)$ changed, both in the above-gap and in the defect-related, subgap spectral region. It can be seen from Fig. 5 that with annealing up to 550°C the true $\alpha(E)$ increased in the region 1.2 to 2.2 eV. In the subgap region, $\alpha(E)$ changed over several orders of magnitude with annealing (Fig. 5). At photon energy 0.8 eV, far below the indirect gap energy, the $\alpha(E)$ increased from the range of 0.06–0.3 to 50–120 cm^{-1}, after anneal at 550°C for 24 h. If we compare the true optical absorption coefficient $\alpha(0.8$ eV$)$ with the ESR spin density of all the 'as-grown' samples, a spin density of 2×10^{16} cm^{-1} corresponds to the

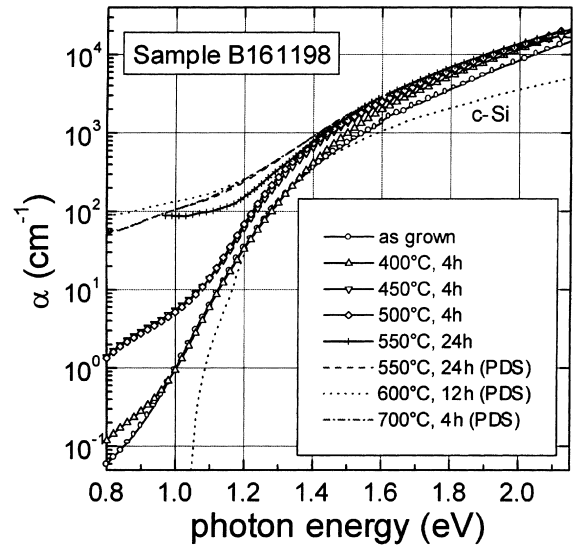

Fig. 5. Optical absorption coefficient spectrum $\alpha(E)$ as a function of photon energy E for μc-Si:H in the 'as-grown' and successively annealed state. Measurement has been done by CPM and T/R except the data marked by PDS. True $\alpha(E)$ has been evaluated with the help of our theory. Single crystalline Si data (c-Si) are shown for comparison.

$\alpha(0.8 \text{ eV}) = 0.12 \text{ cm}^{-1}$. This correspondence is an approximation because there is scatter in the data.

4. Discussion

Raman spectrum and IR absorption monitored structural changes and hydrogen effusion. Raman spectrum can be decomposed into three components. The 480 cm^{-1} component (FWHM about 65 cm^{-1}) is the same as in amorphous silicon (a-Si:H). The peak at 520 cm^{-1} (FWHM 10 cm^{-1}) is nearly two times broader than that of high temperature CVD silicon on saphire and dominates the spectrum. The shoulder around 500 cm^{-1} has been attributed to crystalline grains 2–3 nm size [11]. The area below the 480 cm^{-1} peak is typically 20% of the total area under all bands. The amorphous fraction in the material has to be less because of difference in Raman cross-section of c-Si and a-Si:H and other contributions to this line [12,13].

During annealing in molecular hydrogen atmosphere, changes occur in all the spectra.

Hydrogen leaves the material and new Si dangling bonds are created. Hydrogen desorption can be seen in Fig. 3 at the $\approx$630 cm^{-1} peak, at the doublet between 800 and 900 cm^{-1} and the peak of 2100 cm^{-1}, typical for μc-Si [14]. On the other hand the peak at $\sim$1980 cm^{-1}, originally masked by the 2000 cm^{-1} peak remains unchanged.

Our experimental results support the following '3-phase-model' for μc-Si:H: The first (largest) phase consists of large crystalline nanometer sized grains [5]. The Raman band at 520 cm^{-1} is due to this phase. The second phase has a 'medium disorder' and is a disordered surface layer of grains. Gas adsorption, desorption, and surface reconstruction affect the ESR after effusion of a part of hydrogen from a surface of grains with annealing at 400°C or higher. Resonances with g-values around 2.0055 are assumed to be related to Si dangling bonds in differing environments. Signal around $g = 2.0030$ needs further study. An oxidation (at the air ambient, after the first anneal) can passivate the surface defects (dangling bonds) similar to hydrogenation. Ambient nitrogen gas removes some adsorbed oxygen. The third phase is a residual tissue of amorphous hydrogenated silicon. It's amount decreases by annealing.

Optical properties in the above-gap region can be explained within this model with the effective medium approximation. Larger optical absorption coefficient α (in comparison with crystalline Si) in the region above 2 eV is mainly due to the third phase. The increase in the 1.3–2 eV region is due to the second phase. Hydrogen atoms leave the surface of crystallites and surface states are created.

Comparing defect-related optical absorption and ESR data we observe in the 'as-grown' state a scatter of true α(0.8 eV) but always a similar $g = 2.0055$ signal, which never decreases below 1×10^{16} cm^{-3}, similarly as reported in Ref. [9]. This signal may be partly due to some 'background ESR signal'. On the other hand, α(0.8 eV) after the final annealing is always close to 100 cm^{-1}, but the spin concentration differs by one order of magnitude. Spin concentration does not increase as much as α(0.8 eV) with annealing. The dangling bond occupation may play a role, as deduced from the electrical conductivity changes. It increases up to four orders of magnitude following the 550°C/24 h anneal. Hence, a ratio of doubly (not seen in ESR) to singly occupied Si dangling bonds has changed due to the Fermi level shift. Much more work will be necessary to determine a 'calibration constant' between ESR and defect-connected CPM data, similarly as done in amorphous silicon [15].

5. Conclusions

Besides standard defects with a g-value around 2.0055, new defects (with a g-value around 2.0030) were created during annealing the intrinsic microcrystalline silicon. A three-phase model describes well the structural and optical changes caused by the annealing. Further work is needed to correlate more precisely ESR spin density and subgap optical absorption.

Acknowledgements

The work was supported by the Ministry of Education, Czech Republic, project OK268 and by the Swiss Federal Office of Energy under grant 19431.

References

[1] J. Meier, R. Fluckiger, H. Keppner, A. Shah, Appl. Phys. Lett. 65 (1994) 860.
[2] J. Meier, S. Dubail, R. Fluckiger, D. Fischer, H. Keppner, A. Shah, in: Proceedings of the First WCPSEC, 1994, p. 409.
[3] K. Yamamoto, T. Suzuki, M. Yoshimi, A. Nakajima, in: Proceedings of the 14th EPSEC, 1997, p. 1018.
[4] K. Saito, M. Sano, K. Matuda, T. Kondo, T. Nishimoto, K. Ogawa, I. Kajita, in: Proceedings of the Second WCPSEC, 1999, p. 351.
[5] E. Vallat-Sauvain, U. Kroll, J. Meier, N. Wyrsch, A. Shah, these Proceedings, p. 125.
[6] N. Wyrsch, L. Feitknecht, C. Droz, P. Torres, A. Shah, A. Poruba, M. Vanecek, these Proceedings, p. 1099.
[7] J. Meier, S. Dubail, J. Cuperus, U. Kroll, R. Platz, P. Torres, J.A. Anna Selvan, P. Pernet, N. Beck, N. Pellaton Vaucher, Ch. Hof, D. Fischer, H. Keppner, A. Shah, J. Non-Cryst. Solids 227–230 (1998) 1250.
[8] A. Poruba, A. Fejfar, O. Salyk, M. Vaněček, J. Kočka, presented at 18th Int. Symp. on Amorphous and Microcrystalline Semiconductors, Snowbird, UT, Aug. 1999.
[9] F. Finger, J. Muller, C. Malten, H. Wagner, Phil. Mag. B 77 (1998) 805.

[10] R.A. Street, Hydrogenated Amorphous Silicon, Cambridge University, Cambridge, 1991.
[11] H. Xia, Y.L. He, L.C. Wang, W. Zhang, X.N. Liu, X.K. Zhang, D. Feng, H.E. Jackson, J. Appl. Phys. 78 (1995) 6705.
[12] S. Veprek, F.A. Sarott, Z. Iqbal, Phys. Rev. B 36 (1987) 3344.
[13] L. Houben, M. Luysberg, P. Hapke, R. Carius, F. Finger, H. Wagner, Phil. Mag. B 77 (1998) 1447.
[14] U. Kroll, J. Meier, P. Torres, J. Pohl, A. Shah, J. Non-Cryst. Solids 227–230 (1998) 68.
[15] N. Wyrsch, F. Finger, T.J. McMahon, M. Vaněček, J. Non-Cryst. Solids 137&138 (1991) 347.